The Journal of Chemical Physics

RESEARCH ARTICLE | MAY 15 2023

Implementation of the self-consistent phonons method with *ab initio* potentials (AI-SCP)

Colin Schiltz ; Dmitrij Rappoport ; Vladimir A. Mandelshtam

J. Chem. Phys. 158, 194801 (2023)
https://doi.org/10.1063/5.0146682

The Journal of Chemical Physics ARTICLE scitation.org/journal/jcp

Implementation of the self-consistent phonons method with *ab initio* potentials (AI-SCP)

Cite as: J. Chem. Phys. 158, 194801 (2023); doi: 10.1063/5.0146682
Submitted: 15 February 2023 • Accepted: 24 April 2023 •
Published Online: 15 May 2023

Colin Schiltz,[a] Dmitrij Rappoport, and Vladimir A. Mandelshtam

AFFILIATIONS

Department of Chemistry, University of California, Irvine, California 92697, USA

[a]Author to whom correspondence should be addressed: schiltzc@uci.edu

ABSTRACT

The self-consistent phonon (SCP) method allows one to include anharmonic effects when treating a many-body quantum system at thermal equilibrium. The system is then described by an effective temperature-dependent harmonic Hamiltonian, which can be used to estimate its various dynamic and static properties. In this paper, we combine SCP with *ab initio* (AI) potential energy evaluation in which case the numerical bottleneck of AI-SCP is the evaluation of Gaussian averages of the AI potential energy and its derivatives. These averages are computed efficiently by the quasi-Monte Carlo method utilizing low-discrepancy sequences leading to a fast convergence with respect to the number, S, of the AI energy evaluations. Moreover, a further substantial (an-order-of-magnitude) improvement in efficiency is achieved once a numerically cheap approximation of the AI potential is available. This is based on using a perturbation theory-like (the two-grid) approach in which it is the average of the difference between the AI and the approximate potential that is computed. The corresponding codes and scripts are provided.

I. INTRODUCTION

The self-consistent phonon (SCP) method offers a practical way to improve the harmonic approximation (HA) for computing static and dynamic properties of a general, classical or quantum, many-body system. For a system at thermal equilibrium in a basin of attraction, this variational approach yields the "best" *temperature-dependent* harmonic approximation to the potential energy function (PEF). In essence, it gives the effective harmonic potential, which utilizes the Gibbs–Bogoliubov variational principle for the Helmholtz free energy of the system—meaning the temperature dependence and anharmonic effects are naturally incorporated.

The SCP method was first introduced several decades ago as a means to include anharmonic effects in the approximate treatment of the nuclear dynamics of condensed phase systems.[1,2] The idea of replacing the physical system by a temperature-dependent effective harmonic system is appealing and was later exploited by at least one alternative approach, the principal mode analysis,[3] and has been rediscovered at least once.[4] Note also that in the zero-temperature limit, the variational Gaussian wavepacket method[5] boils down to SCP. Interest in SCP as a practical method to treat finite systems emerged about a decade ago. In Ref. 6, it was used to compute the fundamental frequencies of aromatic hydrocarbons, and in Refs. 7–9, it was used for exploring the size-induced and quantum-induced phase transitions in Lennard-Jones (LJ) clusters. Reference 10 provides a thorough assessment of SCP for computing structural properties of LJ clusters by comparisons to available numerically exact results, concluding that SCP accurately describes the structural properties of LJ clusters in the regime at which the Boltzmann distribution is localized, i.e., when both the thermal and quantum fluctuations are within a basin of attraction of the PEF.

Each quantum dynamics method has its own advantages, but they all share at least one of the following problems. Either the method is approximate or is strictly limited in its applications—with some methods possessing both issues. For example, some exact-in-principle methods scale exponentially with system size (e.g., the basis set methods). Methods such as diffusion Monte Carlo[11,12] or the path integral ground state[13] are limited to ground state calculations, while some *ad hoc* approximate methods (centroid molecular dynamics[14] and ring-polymer molecular dynamics[15,16]) may produce unphysical artifacts that are hard to control. Perturbation theory for a many-body system is often unreliable, complicated numerically, and even determining whether it is suitable for the system at hand is non-trivial. While the harmonic approximation (HA) is manifestly an

approximate method, it is unique in its ability to provide an essentially complete description of a quantum many-body system with a given potential energy for a large class of systems and properties, all without requiring explicit simulation. The shortcomings of HA and the quasiharmonic methods such as SCP are also well documented. For example, the (quasi)harmonic potential does not allow for the correct treatment of multiple-minima potentials or Fermi resonances. Moreover, the HA (and by extension the SCP approximation) suffers from having no generally consistent procedure to systematically improve its accuracy by a gradual increase in computational cost. For example, in order to go beyond the SCP approximation, one needs to make an immense effort. (See Refs. 4 and 17 for examples of such extensions.) These questions are beyond the scope of this paper.

Vibrational self-consistent field (VSCF) and related methods are popular extensions of the HA adding anharmonic corrections in a nonperturbative fashion.[18–21] When coupled with *ab initio* PEFs, the computational bottleneck of VSCF procedures is the energy evaluation, similar to the SCP method. However, the definition of the VSCF wavefunction depends on the basis choice, and for practical reasons, in order to keep the numerical quadrature tractable, the *ab initio* PEF is often replaced by its approximation using a sum of simple products.

Numerically, SCP involves a self-consistent calculation in which at each iteration one needs to compute Gaussian-weighted multivariate integrals of the form

$$\langle f(\mathbf{x})\rangle = \int_{\mathbb{R}^{3N}} \exp\left(-\frac{1}{2}\mathbf{x}^{\mathrm{T}}\mathbf{x}\right) f(\mathbf{x})\, d\mathbf{x}, \tag{1}$$

which is the key numerical bottleneck of the method. Here, $f(\mathbf{x})$ could be associated with the PEF or its gradient. For a pairwise PEF, these integrals can be computed very efficiently by fitting the pair potential as a sum of Gaussians,[22] and this was utilized in, e.g., Ref. 9 for LJ clusters consisting of many thousands of atoms. For a general polyatomic system, a suitable parametrization of the potential is usually unavailable, and due to the high dimensionality, the use of a quadrature is infeasible. Assuming $f(\mathbf{x})$ being a sufficiently smooth function of $\mathbf{x}$, one can evaluate the Gaussian integral (1) numerically using the Monte Carlo (MC) method,

$$\langle f(\mathbf{x})\rangle \approx \frac{1}{S}\sum_{n=1}^{S} f\left(\mathbf{x}^{(n)}\right), \tag{2}$$

where the points $\mathbf{x}^{(n)}$ $(n = 1, \ldots, S)$ are sampled from the Gaussian distribution. Yet, a "naive" approach[6] based on standard MC results in SCP being extremely expensive due to the high accuracy requirement and the slow scaling of the statistical error,

$$\text{error} \sim S^{-1/2} \quad (\text{standard Monte Carlo}), \tag{3}$$

with respect to the number, S, of the grid points and, respectively, the number of gradient evaluations. (Note that here "grid" refers to the quadrature grid associated with the MC sequence.) It was noticed in Ref. 23 that the MC integration can be performed much more efficiently using quasi-MC, which uses deterministic *low-discrepancy* or *quasirandom* sequences (see, e.g., Refs. 24–27 for Sobol sequences) with better uniformity properties. These typically result in a much more favorable scaling of the error with respect to the length of the quasirandom sequence,[28]

$$\text{error} \sim S^{-1} \quad (\text{quasi–Monte Carlo}), \tag{4}$$

and thereby reduce the integration cost by orders of magnitude. This approach, applied to the same aromatic hydrocarbons as in Ref. 6, reduced the computational cost of SCP by several orders of magnitude (e.g., from $\sim 10^{10}$ to $\sim 10^{5}$ gradient evaluations at each iteration), potentially expanding its range of applicability to *ab initio* potentials.

To further reduce the number of energy and gradient evaluations, we consider here a "two-grid approach," which is a perturbation theory-like approach suggested in Ref. 23 specific to the computation of the Gaussian averages of the potential energy and its gradient. The two-grid approach relies on a reference potential $V_{\mathrm{ref}}(\mathbf{r})$, which could be any numerically cheap PEF that reasonably well approximates a presumably accurate (e.g., *ab initio*) but numerically expensive PEF, $V(\mathbf{r})$. Now, consider a Gaussian average (1), e.g., the average potential $\langle V(\mathbf{r})\rangle$. The approximation $V_{\mathrm{ref}}(\mathbf{r})$ does not have to be accurate everywhere but should at least approximate well the rapidly changing terms of $V(\mathbf{r})$, the very terms that define the convergence rate of the numerical integration. By assumption, the average $\langle V_{\mathrm{ref}}(\mathbf{r})\rangle$ is cheap to evaluate on a larger grid of $S' > S$ points. Consequently, we write

$$\langle V(\mathbf{r})\rangle = \langle V_{\mathrm{ref}}(\mathbf{r})\rangle + \langle \Delta V(\mathbf{r})\rangle, \tag{5}$$

where the difference potential $\Delta V(\mathbf{r}) = V(\mathbf{r}) - V_{\mathrm{ref}}(\mathbf{r})$ is by assumption a small and/or slowly varying function of $\mathbf{r}$. Therefore, its average will converge much faster with respect to the length, S, of the quasirandom sequence used for numerical integration. Consequently, in the two-grid approach, the larger grid with S' points is used for evaluating the first term of five, while the evaluation of the second term used a smaller grid of S points. Note also that the perturbation theory-like idea based on using two or more grids of different resolutions and levels of theory has been successfully used by various authors in similar contexts (see, e.g., Refs. 29–39).

Assuming the SCP approximation being a useful extension of the standard HA, the focus of this paper is on its integration with computationally expensive PEFs, in particular, those obtained from *ab initio* quantum chemistry, and consequently using the two-grid approach. In analogy to the previously introduced acronym for *ab initio* Molecular Dynamics (AI-MD),[40] we refer to the present implementation of SCP as AI-SCP. Although the quantum chemistry example (see in the following) uses Density Functional Theory (DFT), our implementation of AI-SCP is very general and can be used with any quantum chemical methods including wavefunction methods.

In Sec. II, we briefly describe the SCP method. We then perform numerical tests, in particular, applying the two-grid approach to two molecular systems: water hexamer, $(H_2O)_6$, represented by one of the best (to date) PEFs (MB-pol[41]) and naphthalene, $C_{10}H_8$, represented by a DFT PEF. These numerical tests will demonstrate that the two-grid approach may lead to about an order of magnitude overall speed-up of the SCP calculation when compared to a single-grid calculation.

II. SELF CONSISTENT PHONONS: BASIC FORMULAS

This section provides a brief but self-contained description of the SCP method.

Consider an N-particle system described by the Hamiltonian

$$\hat{H} = -\frac{\hbar^2}{2}\nabla^{\mathrm{T}}\mathbf{M}^{-1}\nabla + V(\mathbf{r}), \tag{6}$$

where $V(\mathbf{r})$ defines the PEF, $\mathbf{M} = \mathrm{diag}\{m_i\}$ is the mass matrix, and $\mathbf{r} \in \mathbb{R}^{3N}$ is the coordinate vector.

It is assumed that the system is trapped in a local minimum and is at equilibrium at temperature T. We then define a local harmonic approximation

$$\hat{H}_h(T) = -\frac{\hbar^2}{2}\nabla^{\mathrm{T}}\mathbf{M}^{-1}\nabla + V_h(\mathbf{r}), \tag{7}$$

where the harmonic potential is defined by its center $\mathbf{q}$, its value V_0 at the minimum, and the Hessian $\mathbf{K}$,

$$V_h(\mathbf{r}) := \frac{1}{2}(\mathbf{r}-\mathbf{q})^{\mathrm{T}}\mathbf{K}(\mathbf{r}-\mathbf{q}) + V_0. \tag{8}$$

The Gibbs–Bogoliubov inequality,

$$F \le F_{\mathrm{trial}} := F_h + \langle V\rangle_h - \langle V_h\rangle_h, \tag{9}$$

provides an upper limit, F_{trial}, for the free energy, F, of the system, where F_h is the free energy of the harmonic system and the ensemble average, $\langle\cdot\rangle_h := \mathrm{Tr}\,[e^{-\beta\hat{H}_h}\cdot]$, is taken over the Boltzmann distribution of the approximating system defined by the harmonic Hamiltonian $\hat{H}_h$. Minimizing F_{trial} with respect to $\mathbf{q}$, $\mathbf{K}$, and V_0 leads to the following system of coupled nonlinear equations for these parameters:

$$\langle\nabla V\rangle_h = 0, \tag{10a}$$

$$\left\langle\nabla\nabla^{\mathrm{T}}V\right\rangle_h = \mathbf{K}. \tag{10b}$$

Note here that the minimum of the harmonic potential is obtained directly, $V_0 = \langle V\rangle_h$, and the ensemble average (which does not depend on V_0) can be written as

$$\begin{aligned}\langle f(\hat{\mathbf{r}})\rangle_h &:= \mathrm{Tr}\,[e^{-\beta\hat{H}_h}f(\hat{\mathbf{r}})]\\ &= \|2\pi\mathbf{D}\|^{-1/2}\int d\mathbf{x}\, e^{-\frac{1}{2}\mathbf{x}^{\mathrm{T}}\mathbf{D}^{-1}\mathbf{x}}f(\mathbf{q}+\mathbf{x}),\end{aligned} \tag{11}$$

with the displacement–displacement correlation matrix

$$\mathbf{D} = \mathbf{M}^{-1/2}d(\boldsymbol{\Omega})\mathbf{M}^{-1/2} \tag{12}$$

and the auxiliary function

$$d(\omega) := (\hbar/2)\omega^{-1}\coth(\beta\hbar\omega/2). \tag{13}$$

The frequency matrix $\boldsymbol{\Omega}$ is defined via the mass-scaled effective Hessian,

$$\boldsymbol{\Omega}^2 = \tilde{\mathbf{K}} = \mathbf{M}^{-1/2}\mathbf{K}\mathbf{M}^{-1/2}. \tag{14}$$

Many properties of the approximating harmonic system, such as the partition function, fundamental frequencies, free energy, various spatial correlation functions, etc. can be expressed in terms of $\mathbf{q}$, $\mathbf{K}$, and V_0 by numerically evaluating the corresponding Boltzmann average {cf. [Eq. (11)]}.

For the most general case of a quantum system at a finite temperature, the form of Eq. (10a) suggests that their solution must be found iteratively in a self-consistent fashion, e.g., as was performed in Ref. 6 using a procedure akin to the Newton–Raphson algorithm. Namely, given the initial values $\mathbf{q}$ and $\mathbf{K}$, the new values are obtained by implementing the following steps:

$$\mathbf{D}^{(\mathrm{next})} = \mathbf{M}^{-1/2}d(\boldsymbol{\Omega})\mathbf{M}^{-1/2}, \tag{15a}$$

$$\mathbf{K}^{(\mathrm{next})} = \left\langle\nabla\nabla^{\mathrm{T}}V\right\rangle_h, \tag{15b}$$

$$\mathbf{q}^{(\mathrm{next})} = \mathbf{q} - \mathbf{K}^{-1}\langle\nabla V\rangle_h, \tag{15c}$$

where a pseudoinverse (or some kind of regularization) is used for $\mathbf{K}^{-1}$ to handle the singularities of $\mathbf{K}$ and, possibly, some low frequencies. The iteration would continue until the values of $\mathbf{q}$ and $\mathbf{K}$ stop changing. This procedure has superior convergence properties for systems that are not very anharmonic. Unfortunately, it may be unstable if the Hessian matrix $\mathbf{K}$ is ill-conditioned (even after exclusion of the rotational/translational subspace), i.e., if there are highly anharmonic low-frequency vibrational modes. Such is the case for water clusters, which may have some intermolecular degrees of freedom with very low frequencies. For such cases, the following iterative scheme, which is both stable and converges well, was proposed in Ref. 23 and adapted here:

$$\mathbf{K}^{(\mathrm{next})} = \left\langle\nabla\nabla^{\mathrm{T}}V\right\rangle_h, \tag{16a}$$

$$\mathbf{D}^{(\mathrm{next})} = \mathbf{M}^{-1/2}d(\boldsymbol{\Omega})\mathbf{M}^{-1/2}, \tag{16b}$$

$$\mathbf{q}^{(\mathrm{next})} = \mathbf{q} - \tau\mathbf{D}\langle\nabla V\rangle_h, \tag{16c}$$

where τ is an adjustable parameter. (Note that $\mathbf{D}$ is much less ill-conditioned than $\mathbf{K}$.)

III. USING SCP TO COMPUTE FUNDAMENTAL FREQUENCIES AND STRUCTURAL PROPERTIES: NUMERICAL EXAMPLES

In this section, we demonstrate the SCP method to compute the fundamental frequencies and some structural properties of the following two systems.

System I MB-pol water hexamer, i.e., water hexamer $(H_2O)_6$ using one of the best up-to-date PEF (MB-pol)[41] referred to as $V(\mathbf{r})$.

System II TPSSh naphthalene, i.e., naphthalene $C_{10}H_8$ where the electronic energies and gradients at the grid points were evaluated using density functional theory (DFT) with the hybrid TPSSh exchange–correlation functional[42,43] and the resolution-of-the-identity (RI-J) approximation for the Coulomb part.[44] Basis sets of def2-SVP quality[45] and the corresponding auxiliary basis sets[46] were used. To ensure accurate gradients, tighter convergence criteria were applied in the self-consistent field (SCF) procedure. The energy was converged to $10^{-8}E_h$, the density matrix norm to 10^{-8}. All calculations were performed with TURBOMOLE.[47] In our numer-

ical tests, we perform single-grid calculations as well as two-grid calculations according to [Eq. (5)]. The less accurate and cheap PEF, i.e., $V_{\rm ref}(\mathbf{r})$, for System I is q-TIP4P/F[48] and that for System II is the semi-empirical tight-binding (TB) PEF of Van Oanh *et al.*[49]

In Fig. 1, we show a flow chart describing the numerical protocol of a two-grid self-consistent calculation. Note that a single-grid calculation is described by the same flow chart by setting $S = S'$ or $S = 0$ depending on which PEF is used to represent the system (it is always assumed that $S \le S'$). A Python script that interfaces the SCP code with the PEF's codes is provided in the supplementary material together with examples of the required input files and the corresponding source Fortran codes, namely, a single-step SCP code and the program calling the PEFs.

The calculation is initialized using a potential energy minimum of $V(\mathbf{r})$ (not necessarily the global minimum) characterized by the initial (classical) equilibrium structure $\mathbf{q} = \mathbf{q}^{\rm HA}$, the minimum energy $V_0^{\rm HA}$, and the corresponding Hessian matrix $\mathbf{K} = \mathbf{K}^{\rm HA}$ obtained by evaluating the matrix of second derivatives of $V(\mathbf{r})$ at the equilibrium configuration. A single step in the SCP calculation at the iteration number i starts with generating a relatively long Sobol sequence $\{\mathbf{r}^{(n)}\}$ $(n = 1, \ldots, S')$ distributed according to Eqs. (2) and (11). These points are then used as the input for the codes computing the energies and gradients of $V(\mathbf{r}^{(n)})$ $(n = 1, \ldots, S)$ and $V_{\rm ref}(\mathbf{r}^{(n)})$ $(n = 1, \ldots, S')$ with S being generally much smaller than S' and evaluating the averages that appear in the RHSs of Eq. (15) and needed to compute the new harmonic pair $(\mathbf{q}, \mathbf{K})$. The iteration continues while gradually increasing S with S' being fixed. The convergence is monitored, e.g., by inspection of the behavior of the fundamental frequencies as a function of the iteration number i. Note that the Sobol sequences used at different iteration steps are never the same. This allows one to estimate the statistical errors caused by the finite values of S and S' for the computed properties by comparing results at different iteration steps.

A. System I: Water hexamer, $(H_2O)_6$

Water hexamer has received considerable attention in the past, both experimentally and theoretically.[23,50–71] The most recent publications indicate continuing interest in this system.[72–74] One reason is that six is the smallest number of water molecules that can arrange themselves in stable three-dimensional structures. Such structures have even acquired their own names: "prism," "cage," "book," etc. There have been numerous attempts to produce an accurate and efficient PEF for water; the most recent and successful ones are MB-pol from Babin *et al.*[41] and q-AQUA from Yu *et al.*[75] While being much cheaper than the *ab initio* energies, these latter PEFs are still numerically expensive when compared to some popular empirical PEFs, such as q-TIP4P/F.[48] Our goal here is, in particular, to investigate the possibility of using an accurate and expensive PEF $V(\mathbf{r})$ (MB-pol[41] in the present demonstration) and a cheap PEF (q-TIP4P/F[48]) referred to as $V_{\rm ref}(\mathbf{r})$ in the framework of the two-grid SCP calculation {cf. [Eq. (5)]}.

In Fig. 2, we show a typical result for the MB-pol hexamer prism using a single-grid protocol and following a particular grid size schedule, i.e., the $S = S(i)$ dependence, where i stands for the

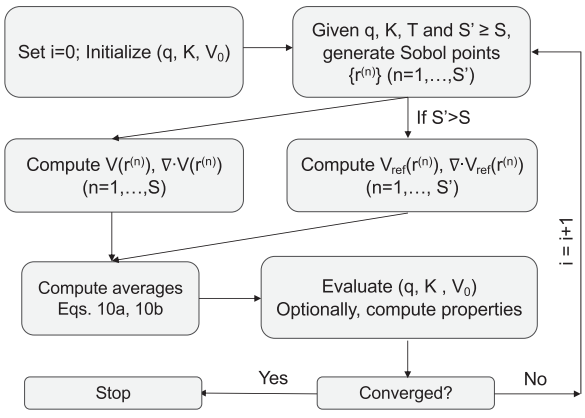

FIG. 1. The flow chart of a two-grid SCP calculation.

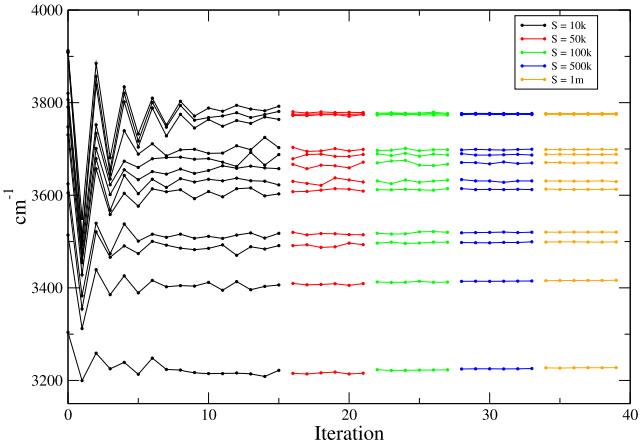

FIG. 2. The OH stretch fundamental frequencies of the MB-pol hexamer prism at $T = 0$, computed by the SCP method using a single grid for integration. The frequencies are shown as a function of the iteration number. Different colors correspond to different numbers of points, S, in the Sobol sequence used to compute the Gaussian integrals.

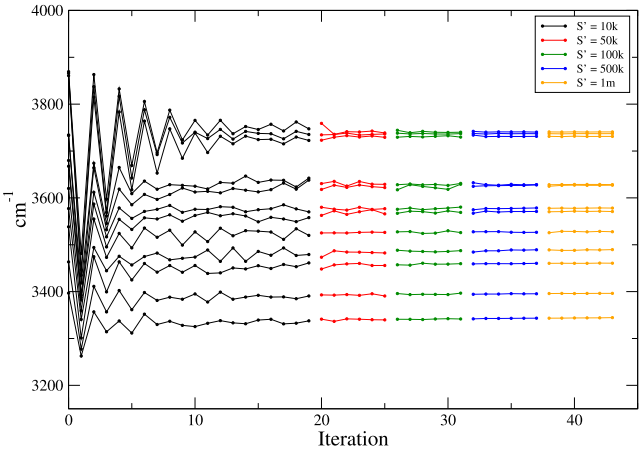

FIG. 3. Same as Fig. 2 but for the q-TIP4P/F hexamer prism.

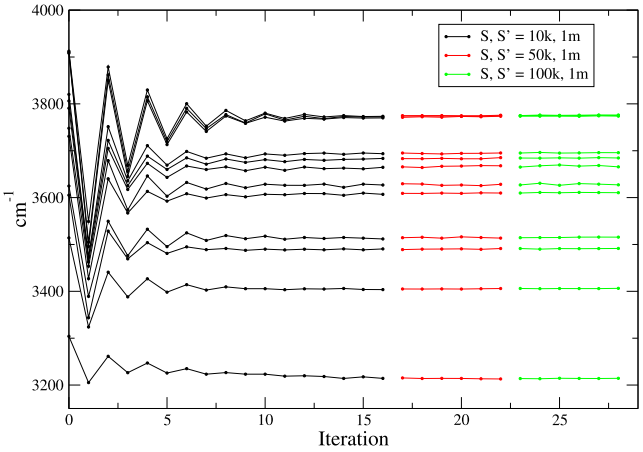

FIG. 4. Two-grid SCP calculation at $T = 0$ for the MB-pol hexamer prism. S and S' indicate the numbers of gradient evaluations for, respectively, MB-pol and q-TIP4P/F PEFs.

iteration number. The S values are indicated in the figure. Similarly, Fig. 3 shows a typical result for the q-TIP4P/F hexamer prism, and Fig. 4 shows a typical result for the MB-pol hexamer prism using a two-grid SCP calculation with the size of the "cheap" grid $S' = 10^6$ fixed. In Fig. 5, we show results using another possible grid size schedule that could be advantageous in which the grid size is increasing gradually according to

$$S = (10^5 - 10^3) \times (0.02i)^2. \tag{17}$$

Note although that no additional optimization of the grid size schedule has been performed. However, it is clear that an optimal schedule depends on the system and, in particular, may be difficult to devise for a complex system with large dynamic range (such as water clusters) without tests involving a cheap reference system with similar properties.

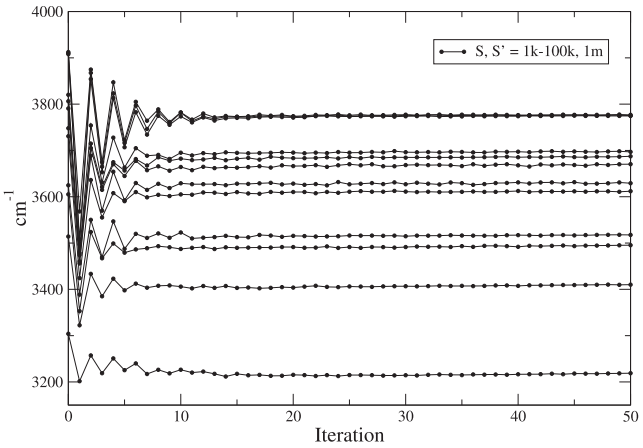

FIG. 5. Two-grid SCP calculation for the MB-pol hexamer prism as in Fig. 4 but using the quadratic schedule $S = (10^5 - 10^3) \times (0.02i)^2$ $(i = 1, \ldots, 50)$ with fixed $S' = 10^6$.

The statistical errors caused by the finite sizes of the Monte Carlo sequences used to evaluate the Gaussian integrals can be estimated directly from the behavior of the computed fundamental frequencies as a function of the iteration number i. Here, in order to obtain more accurate information on the errors for the fundamental frequencies as a function of the grid size (i.e., the number of the gradient evaluations at the last iteration) we performed the calculations implementing a very large grid, $S = 2.5 \times 10^6$. The corresponding errors averaged over the 12 OH stretch frequencies as functions of the grid sizes for the specified three cases are shown in Fig. 6. The error averaged over all the $(3N - 6)$ fundamental frequencies $(N = 18)$ is shown in Fig. 7. Apparently, the latter is smaller, i.e., the smaller the frequency the smaller the statistical error. Figure 8 shows that the convergence behavior is consistent between the fundamental frequencies and the calculated Helmholtz free energy. The following observations are in order. First, the error is approximately linear with respect to the inverse grid size, i.e., $1/S$, which is a manifestation of the very property of quasi-MC integration that makes it superior to the standard, i.e., Metropolis, MC. Second, note that q-TIP4P/F, i.e., the cheap auxiliary potential $V_{\mathrm{ref}}(\mathbf{r})$, was not specifically designed to approximate the accurate MB-pol PEF. Indeed, while the latter is an accurate fit to the *ab initio* data, the former was an empirical PEF adjusted to reproduce certain thermodynamic properties of water.[48] Yet, the present results demonstrate that a substantial reduction in the number of the expensive gradient evaluations can still be achieved. Clearly, with the idea of approximating accurately $V(\mathbf{r})$ only in the regions of its most "wild" behavior (i.e., where its gradient and/or the Hessian are large), much better choices could be made, thus leading to even more significant speed-ups.

Once the optimal harmonic Hamiltonian is obtained, various properties, besides the fundamental frequencies, could be computed. Some of those are reported in Tables I and II, i.e., respectively, the

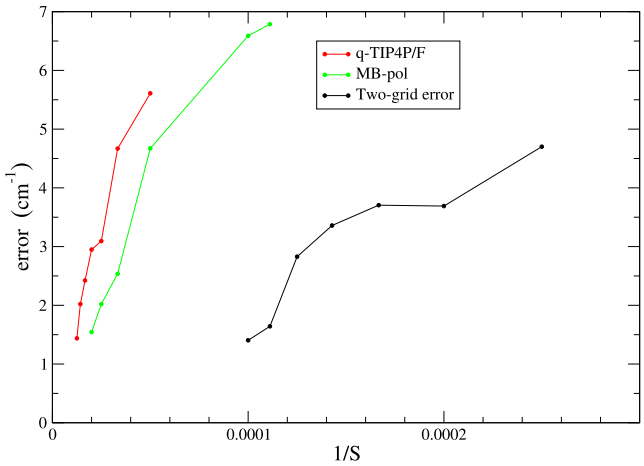

FIG. 6. The error for the computed fundamental frequencies of the hexamer prism averaged over the 12 OH stretch modes as a function of $1/S$. The errors were computed by taking the difference with the frequencies computed using $S = 2.5 \times 10^6$. Red line: using a single-grid SCP calculation for the q-TIP4P/F hexamer. Green line: same for the MB-pol hexamer. Black line: using a two-grid SCP calculation for the MB-pol hexamer. S and S' indicate the numbers of gradient evaluations for, respectively, MB-pol and q-TIP4P/F PEFs.

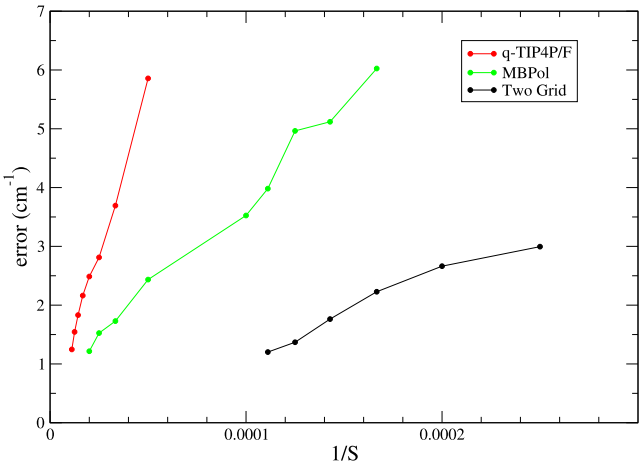

FIG. 7. Same as Fig. 6 but averaged over all the $(3N-6)$ fundamental frequencies of the water hexamer.

TABLE I. The H–O–H bond angles θ_{HOH} (in degrees) for the six monomers in the MB-pol hexamer prism from the corresponding minimum of the MB-pol PEF (left column) and the quantum anharmonic corrections $\Delta\theta_{HOH}$ at $T = 0$ from a converged SCP calculation (right column).

HA	SCP
106.78	0.16
106.42	0.22
102.15	0.19
101.34	0.13
104.41	0.19
106.21	0.20

TABLE II. The O–O distances R_{OO} (in Angstroms) for all monomer–monomer pairs in the minimum of the MB-pol hexamer prism (upper triangle) and the quantum anharmonic corrections, $\Delta R_{O_iO_j}$, at $T = 0$ from a converged SCP calculation (lower triangle).

HA SCP	1	2	3	4	5	6
1		2.775	2.886	2.918	2.662	3.931
2	0.006		3.834	3.956	2.923	3.914
3	0.008	0.008		2.801	4.084	4.223
4	0.009	0.008	0.007		2.743	2.907
5	0.003	0.006	0.009	0.005		2.933
6	0.008	0.007	0.011	0.008	0.008	

H–O–H bond angles, θ_{HOH}, and O–O distances, R_{OO}, in the prism isomer at $T = 0$ (i.e., for its ground vibrational state). Note that the data are shown for the prism minimum of the MB-pol PEF, while the SCP results are given in terms of the shifts, i.e., respectively, $\Delta\theta_{HOH}$ and ΔR_{OO}. Table III contains further information pertinent to the method.

TABLE III. Fundamental frequencies (cm^{-1}) of CH stretch modes of TB naphthalene and naphthalene represented by the TPSSh functional with the def2-SVP basis from harmonic approximation (HA) and the frequency shift for a converged SCP calculation.

Mode	TB, HA	TB, SCP	TPSSh, HA	TPSSh, SCP
1	3130	−91	3200	−39
2	3127	−88	3198	−45
3	3126	−91	3188	−41
4	3123	−88	3186	−47
5	3117	−91	3175	−46
6	3116	−90	3173	−53
7	3112	−88	3168	−65
8	3111	−88	3167	−83

B. System II: Naphthalene, $C_{10}H_8$

The CH stretch IR spectra of aromatic hydrocarbons were studied before, specifically, using the SCP method in Ref. 6. Yet, this implementation of SCP would rather seem discouraging as it appeared to be extremely expensive because of the $\sim S^{-1/2}$ convergence of the MC integration. The quasi-MC approach introduced later in Ref. 23 already resulted in several orders of magnitude reduction in the computational time. However, in order to reduce the statistical errors for the CH fundamental frequencies to about 1/cm, the cost of each iteration would be about 10^5 gradient evaluations (see in the following), which is already feasible using *ab initio* PEF but still very expensive. Here, as in Subsection III A, we use the two-grid approach to demonstrate that the latter provides another order of magnitude reduction in the computational cost, thus making AI-SCP even more practical.

Due to the small dynamic range (the absence of weak intermolecular modes), the "Newton–Raphson" iterative scheme (15) is stable for this weakly anharmonic system, requiring a small (i.e., ~10) number of iterations to converge all the fundamental frequencies (Fig. 8).[6]

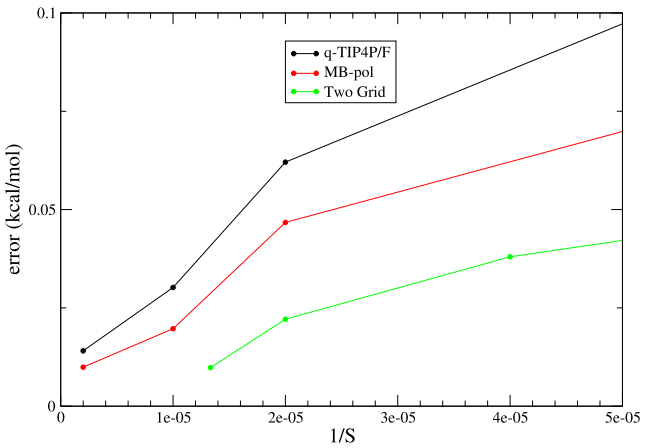

FIG. 8. Same as Fig. 6 but for the Helmholtz free energy, which at $T = 0$ is equal to the ground state energy of the optimal harmonic system as obtained by SCP.

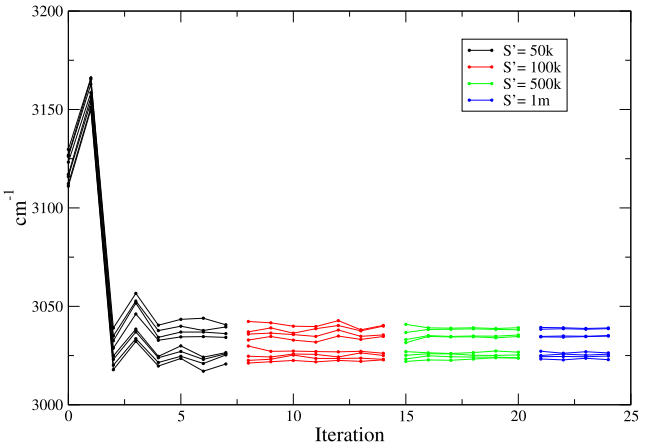

FIG. 9. An example of a single-grid SCP calculation at $T = 0$ for naphthalene represented by the TB PEF[49] following a particular schedule and showing the CH stretch fundamental frequencies as a function of the iteration number.

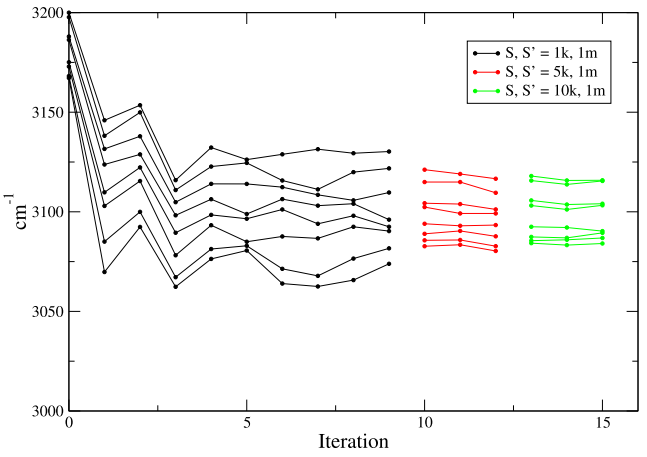

FIG. 10. An example of a two-grid SCP calculation at $T = 0$ for naphthalene represented by the DFT PEF using the TPSSh functional.[42,43] The TB potential[49] was used for the reference PEF.

To this end, Fig. 9 shows the CH fundamental frequencies as a function of the iteration number for the reference system, TB naphthalene, using a possible (not necessarily optimal) grid size schedule as indicated in the figure. Figure 10 shows the results of a two-grid calculation for the TPSSh naphthalene. We also performed much more accurate two-grid SCP calculation using as many as $S = 4 \times 10^4$ Sobol points. As before, this latter calculation was used to estimate the statistical errors for the CH frequencies as a function of S. The errors averaged over the eight CH stretch frequencies are shown in Fig. 11, while those averaged over all the $(3N - 6)$ frequencies $(N = 18)$ are shown in Fig. 11. Here, again, we observe that the statistical errors are the largest for the highest frequencies that the CH frequencies are. The comparison with the errors from a single-grid SCP calculation for the reference system, i.e., the TB naphthalene is

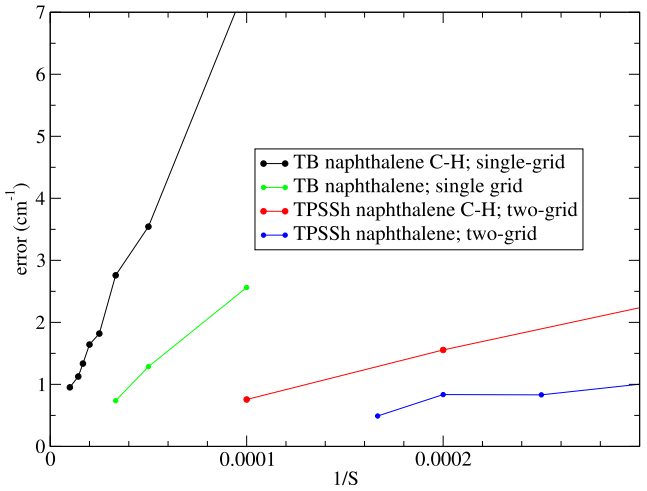

FIG. 11. The errors for the computed fundamental frequencies of naphthalene averaged over the eight CH stretch modes as a function of $1/S$ and over all the $(3N - 6)$ fundamental frequencies of naphthalene. The errors were computed by taking the difference with the frequencies computed using $S = 10^6$ for the TB naphthalene (single-grid SCP) and $S = 4 \times 10^4$; $S' = 10^6$, for the TPSSh naphthalene (two-grid SCP).

striking. An order of magnitude reduction in the number of gradient evaluations for the expensive *ab initio* PEF is apparent from the figure.

IV. CONCLUSIONS

In this paper, we revisited the SCP method.[1,2,4,6] The method is based on approximating a molecular system localized in a basin of attraction using an optimal temperature-dependent harmonic approximation. Given the optimal harmonic Hamiltonian, one can then estimate various dynamic and static properties of such a system with anharmonic effects included implicitly in a conceptually simple and straightforward fashion. Due to a number of algorithmic breakthroughs proposed in Ref. 23, the method was made numerically very efficient. Here, we applied SCP to two challenging systems, a naphthalene molecule and water hexamer cluster, and demonstrated that the method is practical, even when used with a DFT potential. A key prerequisite for the most numerically efficient implementation of the method is the availability of a cheap approximation of the accurate PEF. Although not strictly *ab initio* potentials have been used in the present numerical demonstrations, the two-grid approach may be combined with other empirical or *ab initio* PEFs for better performance. The method has been interfaced with an electronic-structure package (TURBOMOLE). The corresponding Python scripts and FORTRAN source codes have been made available.

SUPPLEMENTARY MATERIAL

The Fortran source codes and Python scripts for interfacing AI-SCP with quantum chemistry methods are linked in the supplementary material.

ACKNOWLEDGMENTS

We would like to thank Filipp Furche for useful discussions. Marc Riera-Riambau is thanked for help with the source code for the MB-pol PEF. This work was supported by the National Science Foundation (NSF) Grant No. CHE-1900295.

AUTHOR DECLARATIONS

Conflict of Interest

The authors have no conflicts to disclose.

Author Contributions

Colin Schiltz: Conceptualization (supporting); Data curation (lead); Formal analysis (supporting); Investigation (lead); Methodology (equal); Software (lead); Validation (equal); Visualization (lead); Writing – original draft (supporting); Writing – review & editing (lead). **Dmitrij Rappoport**: Data curation (equal); Investigation (equal); Methodology (equal); Validation (equal); Writing – review & editing (equal). **Vladimir A. Mandelshtam**: Conceptualization (lead); Formal analysis (lead); Funding acquisition (lead); Investigation (supporting); Methodology (equal); Resources (lead); Supervision (lead); Validation (equal); Visualization (supporting); Writing – original draft (lead); Writing – review & editing (supporting).

DATA AVAILABILITY

The data that support the findings of this study are available from the corresponding author upon reasonable request.

REFERENCES

[1] T. R. Koehler, "Theory of the self-consistent harmonic approximation with application to solid neon," Phys. Rev. Lett. **17**, 89–91 (1966).
[2] N. S. Gillis, N. R. Werthamer, and T. R. Koehler, "Properties of crystalline argon and neon in the self-consistent phonon approximation," Phys. Rev. **165**, 951–959 (1968).
[3] B. R. Brooks, D. Janežič, and M. Karplus, "Harmonic analysis of large systems. I. Methodology," J. Comput. Chem. **16**, 1522–1542 (1995).
[4] J. Cao and G. A. Voth, "Modeling physical systems by effective harmonic oscillators: The optimized quadratic approximation," J. Chem. Phys. **102**, 3337–3348 (1995).
[5] P. A. Frantsuzov and V. A. Mandelshtam, "Effects of quantum delocalization on structural changes of Lennard-Jones clusters," J. Chem. Phys. **121**, 9247–9256 (2004).
[6] F. Calvo, P. Parneix, and N.-T. Van-Oanh, "Finite-temperature infrared spectroscopy of polycyclic aromatic hydrocarbon molecules. II. Principal mode analysis and self-consistent phonons," J. Chem. Phys. **133**, 074303 (2010).
[7] J. Deckman and V. A. Mandelshtam, "Effects of quantum delocalization on structural changes of Lennard-Jones clusters," J. Phys. Chem. **113**, 7394 (2009).
[8] I. Georgescu and V. A. Mandelshtam, "A fast variational Gaussian wavepacket method: Size-induced structural transitions in large neon clusters," J. Chem. Phys. **135**, 154106 (2011).
[9] I. Georgescu and V. A. Mandelshtam, "Self-consistent phonons revisited. I. The role of thermal versus quantum fluctuations on structural transitions in large Lennard-Jones clusters," J. Chem. Phys. **137**, 144106 (2012).
[10] S. E. Brown and V. A. Mandelshtam, "Self-consistent phonons: An accurate and practical method to account for anharmonic effects in equilibrium properties of general classical or quantum many-body systems," Chem. Phys. **481**, 69–76 (2016).
[11] J. B. Anderson, "A random-walk simulation of the Schrödinger equation: H_3^+," J. Chem. Phys. **63**, 1499–1503 (1975).
[12] J. B. Anderson, "Quantum chemistry by random walk. H^2P, H_3^+ D_{3h} $^1A_1'$, H_2 $^3\Sigma_u^+$, H_4 $^1\Sigma_g^+$, Be ^1S," J. Chem. Phys. **65**, 4121–4127 (1976).
[13] A. Sarsa, K. E. Schmidt, and W. R. Magro, "A path integral ground state method," J. Chem. Phys. **113**, 1366–1371 (2000).
[14] J. Cao and G. A. Voth, "A new perspective on quantum time correlation functions," J. Chem. Phys. **99**, 10070 (1993).
[15] I. R. Craig and D. E. Manolopoulos, "Quantum statistics and classical mechanics: Real time correlation functions from ring polymer molecular dynamics," J. Chem. Phys. **121**, 3368 (2004).
[16] B. J. Braams and D. E. Manolopoulos, "On the short-time limit of ring polymer molecular dynamics," J. Chem. Phys. **125**, 124105 (2006).
[17] I. Georgescu, S. Jitomirskaya, and V. A. Mandelshtam, "On the ground state calculation of a many-body system using a self-consistent basis and quasi-Monte Carlo: An application to water hexamer," J. Chem. Phys. **139**, 204104 (2013).
[18] J. M. Bowman, "Self-consistent field energies and wavefunctions for coupled oscillators," J. Chem. Phys. **68**, 608–610 (1978).
[19] G. D. Carney, L. L. Sprandel, and C. W. Kern, "Variational approaches to vibration-rotation spectroscopy for polyatomic molecules," in *Advances in Chemical Physics*, edited by I. Prigogine and S. A. Rice (Wiley, New York, 1978), Vol. 37, Chap. 6, pp. 305–379.
[20] R. B. Gerber and M. A. Ratner, "A semiclassical self-consistent field (SC SCF) approximation for eigenvalues of coupled-vibration systems," Chem. Phys. Lett. **68**, 195–198 (1979).
[21] T. K. Roy and R. B. Gerber, "Vibrational self-consistent field calculations for spectroscopy of biological molecules: New algorithmic developments and applications," Phys. Chem. Chem. Phys. **15**, 9468–9492 (2013).
[22] N. Corbin and K. Singer, "Semiclassical molecular dynamics of wave packets," Mol. Phys. **46**, 671–677 (1982).
[23] S. E. Brown, I. Georgescu, and V. A. Mandelshtam, "Self-consistent phonons revisited. II. A general and efficient method for computing free energies and vibrational spectra of molecules and clusters," J. Chem. Phys. **138**, 044317 (2013).
[24] I. M. Sobol, "On the distribution of points in a cube and the approximate evaluation of integrals," USSR Comput. Math. Math. Phys. **7**, 86–112 (1967).
[25] I. M. Sobol, "Uniformly distributed sequences with an additional uniform property," USSR Comput. Math. Math. Phys. **16**, 236–242 (1976).
[26] W. J. Morokoff and R. E. Caflisch, "Quasi-random sequences and their discrepancies," SIAM J. Sci. Comput. **15**, 1251–1279 (1994).
[27] W. J. Morokoff and R. E. Caflisch, "Quasi-Monte Carlo integration," J. Comput. Phys. **122**, 218–230 (1995).
[28] R. Schürer, "A comparison between (quasi-)Monte Carlo and cubature rule based methods for solving high-dimensional integration problems," Math. Comput. Simul. **62**, 509–517 (2003).
[29] B. Hetényi, K. Bernacki, and B. J. Berne, "Multiple 'time step' Monte Carlo," J. Chem. Phys. **117**, 8203–8207 (2002).
[30] T. E. Markland and D. E. Manolopoulos, "A refined ring polymer contraction scheme for systems with electrostatic interactions," Chem. Phys. Lett. **464**, 256–261 (2008).
[31] O. Marsalek and T. E. Markland, "*Ab initio* molecular dynamics with nuclear quantum effects at classical cost: Ring polymer contraction for density functional theory," J. Chem. Phys. **144**, 054112 (2016).
[32] V. Kapil, J. VandeVondele, and M. Ceriotti, "Accurate molecular dynamics and nuclear quantum effects at low cost by multiple steps in real and imaginary time: Using density functional theory to accelerate wavefunction methods," J. Chem. Phys. **144**, 054111 (2016).
[33] X. Cheng, J. D. Herr, and R. P. Steele, "Accelerating *ab initio* path integral simulations via imaginary multiple-timestepping," J. Chem. Theory Comput. **12**, 1627–1638 (2016).
[34] Y. Xue, J.-N. Wang, W. Hu, J. Zheng, Y. Li, X. Pan, Y. Mo, Y. Shao, L. Wang, and Y. Mei, "Affordable *ab initio* path integral for thermodynamic properties via molecular dynamics simulations using semiempirical reference potential," J. Phys. Chem. A **125**, 10677–10685 (2021).
[35] G. Rauhut, "Efficient calculation of potential energy surfaces for the generation of vibrational wave functions," J. Chem. Phys. **121**, 9313–9322 (2004).

[36]K. Yagi, S. Hirata, and K. Hirao, "Multiresolution potential energy surfaces for vibrational state calculations," Theor. Chem. Acc. **118**, 681–691 (2007).
[37]D. M. Benoit, "Fast vibrational calculation of anharmonic OH-stretch frequencies for two low-energy noradrenaline conformers," J. Chem. Phys. **129**, 234304 (2008).
[38]M. Sparta, I.-M. Høyvik, D. Toffoli, and O. Christiansen, "Potential energy surfaces for vibrational structure calculations from a multiresolution adaptive density-guided approach: Implementation and test calculations," J. Phys. Chem. A **113**, 8712–8723 (2009).
[39]T. K. Roy and R. B. Gerber, "Dual basis approach for ab initio anharmonic calculations of vibrational spectroscopy: Application to microsolvated biomolecules," J. Chem. Theory Comput. **16**, 7005–7016 (2020).
[40]R. Car and M. Parrinello, "Unified approach for molecular dynamics and density-functional theory," Phys. Rev. Lett. **55**, 2471–2474 (1985).
[41]V. Babin, G. R. Medders, and F. Paesani, "Development of a 'first principles' water potential with flexible monomers. II: Trimer potential energy surface, third virial coefficient, and small clusters," J. Chem. Theory Comput. **10**, 1599–1607 (2014).
[42]V. N. Staroverov, G. E. Scuseria, J. Tao, and J. P. Perdew, "Erratum: 'Comparative assessment of a new nonempirical density functional: Molecules and hydrogen-bonded complexes' [J. Chem. Phys. 119, 12129 (2003)]," J. Chem. Phys. **121**, 11507 (2004).
[43]V. N. Staroverov, G. E. Scuseria, J. Tao, and J. P. Perdew, "Comparative assessment of a new nonempirical density functional: Molecules and hydrogen-bonded complexes," J. Chem. Phys. **119**, 12129–12137 (2003).
[44]K. Eichkorn, O. Treutler, H. Öhm, M. Häser, and R. Ahlrichs, "Auxiliary basis sets to approximate Coulomb potentials (Chem. Phys. Letters 240 (1995) 283-290)," Chem. Phys. Lett. **242**, 652–660 (1995).
[45]F. Weigend and R. Ahlrichs, "Balanced basis sets of split valence, triple zeta valence and quadruple zeta valence quality for H to Rn: Design and assessment of accuracy," Phys. Chem. Chem. Phys. **7**, 3297–3305 (2005).
[46]F. Weigend, "Accurate Coulomb-fitting basis sets for H to Rn," Phys. Chem. Chem. Phys. **8**, 1057–1065 (2006).
[47]S. G. Balasubramani, G. P. Chen, S. Coriani, M. Diedenhofen, M. S. Frank, Y. J. Franzke, F. Furche, R. Grotjahn, M. E. Harding, C. Hättig, A. Hellweg, B. Helmich-Paris, C. Holzer, U. Huniar, M. Kaupp, A. Marefat Khah, S. Karbalaei Khani, T. Müller, F. Mack, B. D. Nguyen, S. M. Parker, E. Perlt, D. Rappoport, K. Reiter, S. Roy, M. Rückert, G. Schmitz, M. Sierka, E. Tapavicza, D. P. Tew, C. van Wüllen, V. K. Voora, F. Weigend, A. Wodyński, and J. M. Yu, "TURBOMOLE: Modular program suite for *ab initio* quantum-chemical and condensed-matter simulations," J. Chem. Phys. **152**, 184107 (2020).
[48]S. Habershon, T. E. Markland, and D. E. Manolopoulos, "Competing quantum effects in the dynamics of a flexible water model," J. Chem. Phys. **131**, 024501 (2009).
[49]N.-T. Van-Oanh, P. Parneix, and P. Bréchignac, "Vibrational dynamics of the neutral naphthalene molecule from a tight-binding approach," J. Phys. Chem. A **106**, 10144–10151 (2002).
[50]R. N. Pribble and T. S. Zwier, "Size-specific infrared-spectra of benzene-$(H_2O)_n$ clusters (n = 1 through 7): Evidence for noncyclic $(H_2O)_n$ structures," Science **265**, 75–79 (1994).
[51]K. Liu, M. G. Brown, C. Carter, R. J. Saykally, J. K. Gregory, and D. C. Clary, "Characterization of a cage form of the water hexamer," Nature **381**, 501–503 (1996).
[52]E. S. Kryachko, "Ab initio studies of the conformations of water hexamer: Modelling the penta-coordinated hydrogen-bonded pattern in liquid water," Chem. Phys. Lett. **314**, 353–363 (1999).
[53]K. Nauta and R. E. Miller, "Formation of cyclic water hexamer in liquid helium: The smallest piece of ice," Science **287**, 293–295 (2000).
[54]M. Losada and S. Leutwyler, "Water hexamer clusters: Structures, energies, and predicted mid-infrared spectra," J. Chem. Phys. **117**, 2003–2016 (2002).
[55]C. Steinbach, P. Andersson, M. Melzer, J. K. Kazimirski, U. Buck, and V. Buch, "Detection of the book isomer from the OH-stretch spectroscopy of size selected water hexamers," Phys. Chem. Chem. Phys. **6**, 3320–3324 (2004).
[56]M. E. Dunn, E. K. Pokon, and G. C. Shields, "Thermodynamics of forming water clusters at various temperatures and pressures by Gaussian-2, Gaussian-3, complete basis set-QB3, and complete basis set-APNO model chemistries; implications for atmospheric chemistry," J. Am. Chem. Soc. **126**, 2647–2653 (2004).
[57]E. E. Dahlke, R. M. Olson, H. R. Leverentz, and D. G. Truhlar, "Assessment of the accuracy of density functionals for prediction of relative energies and geometries of low-lying isomers of water hexamers," J. Phys. Chem. A **112**, 3976–3984 (2008).
[58]D. M. Bates and G. S. Tschumper, "CCSD(T) complete basis set limit relative energies for low-lying water hexamer structures," J. Phys. Chem. A **113**, 3555–3559 (2009).
[59]Y. Wang, X. Huang, B. C. Shepler, B. J. Braams, and J. M. Bowman, "Flexible, *ab initio* potential, and dipole moment surfaces for water. I. Tests and applications for clusters up to the 22-mer," J. Chem. Phys. **134**, 094509 (2011).
[60]Y. Wang and J. M. Bowman, "*Ab initio* potential and dipole moment surfaces for water. II. Local-monomer calculations of the infrared spectra of water clusters," J. Chem. Phys. **134**, 154510 (2011).
[61]C. Pérez, M. T. Muckle, D. P. Zaleski, N. A. Seifert, B. Temelso, G. C. Shields, Z. Kisiel, and B. H. Pate, "Structures of cage, prism, and book isomers of water hexamer from broadband rotational spectroscopy," Science **336**, 897–901 (2012).
[62]Y. Wang, V. Babin, J. M. Bowman, and F. Paesani, "The water hexamer: Cage, prism, or both. Full dimensional quantum simulations say both," J. Am. Chem. Soc. **134**, 11116–11119 (2012).
[63]R. J. Saykally and D. J. Wales, "Pinning down the water hexamer," Science **336**, 814–815 (2012).
[64]C. J. Tainter and J. L. Skinner, "The water hexamer: Three-body interactions, structures, energetics, and OH-stretch spectroscopy at finite temperature," J. Chem. Phys. **137**, 104304 (2012).
[65]J. O. Richardson, C. Pérez, S. Lobsiger, A. A. Reid, B. Temelso, G. C. Shields, Z. Kisiel, D. J. Wales, B. H. Pate, and S. C. Althorpe, "Concerted hydrogen-bond breaking by quantum tunneling in the water hexamer prism," Science **351**, 1310–1313 (2016).
[66]S. E. Brown, A. W. Götz, X. Cheng, R. P. Steele, V. A. Mandelshtam, and F. Paesani, "Monitoring water clusters 'melt' through vibrational spectroscopy," J. Am. Chem. Soc. **139**, 7082–7088 (2017).
[67]W. T. S. Cole, Ö. Yönder, A. A. Sheikh, R. S. Fellers, M. R. Viant, R. J. Saykally, J. D. Farrell, and D. J. Wales, "Terahertz VRT spectroscopy of the water hexamer-h12 cage: Dramatic libration-induced enhancement of hydrogen bond tunneling dynamics," J. Phys. Chem. A **122**, 7421–7426 (2018).
[68]W. T. S. Cole, J. D. Farrell, A. A. Sheikh, Ö. Yönder, R. S. Fellers, M. R. Viant, D. J. Wales, and R. J. Saykally, "Terahertz VRT spectroscopy of the water hexamer-d_{12} prism: Dramatic enhancement of bifurcation tunneling upon librational excitation," J. Chem. Phys. **148**, 094301 (2018).
[69]E. Lambros and F. Paesani, "How good are polarizable and flexible models for water: Insights from a many-body perspective," J. Chem. Phys. **153**, 060901 (2020).
[70]A. Nandi, C. Qu, P. L. Houston, R. Conte, Q. Yu, and J. M. Bowman, "A CCSD(T)-based 4-body potential for water," J. Phys. Chem. Lett. **12**, 10318–10324 (2021).
[71]R. J. DiRisio, J. M. Finney, and A. B. McCoy, "Diffusion Monte Carlo approaches for studying nuclear quantum effects in fluxional molecules," Wiley Interdiscip. Rev.: Comput. Mol. Sci. **12**, e1615 (2022).
[72]V. G. M. Lee, N. J. Vetterli, M. A. Boyer, and A. B. McCoy, "Diffusion Monte Carlo studies on the detection of structural changes in the water hexamer upon isotopic substitution," J. Phys. Chem. A **124**, 6903–6912 (2020).
[73]K. Sharkas, K. Wagle, B. Santra, S. Akter, R. R. Zope, T. Baruah, K. A. Jackson, J. P. Perdew, and J. E. Peralta, "Self-interaction error overbinds water clusters but cancels in structural energy differences," Proc. Natl. Acad. Sci. U. S. A. **117**, 11283–11288 (2020).
[74]S. Jana, L. A. Constantin, and P. Samal, "Accurate water properties from an efficient ab initio method," J. Chem. Theory Comput. **16**, 974–987 (2020).
[75]Q. Yu, C. Qu, P. L. Houston, R. Conte, A. Nandi, and J. M. Bowman, "q-AQUA: A many-body CCSD(T) water potential, including four-body interactions, demonstrates the quantum nature of water from clusters to the liquid phase," J. Phys. Chem. Lett. **13**, 5068–5074 (2022).